ENVIRONMENTAL RESEARCH
LETTERS

LETTER • OPEN ACCESS

Regional projection of climate warming effects on coastal seas in east China

To cite this article: Wenxia Zhang *et al* 2022 *Environ. Res. Lett.* **17** 074006

ENVIRONMENTAL RESEARCH
LETTERS

OPEN ACCESS

RECEIVED
29 December 2021

REVISED
10 May 2022

ACCEPTED FOR PUBLICATION
25 May 2022

PUBLISHED
16 June 2022

LETTER

Regional projection of climate warming effects on coastal seas in east China

Wenxia Zhang[1,2,*], **John P Dunne**[3], **Hui Wu**[1] and **Feng Zhou**[2]

[1] State Key Laboratory of Estuarine and Coastal Research, Institute of Eco-Chongming, East China Normal University, Shanghai, People's Republic of China
[2] State Key Laboratory of Satellite Ocean Environment Dynamics, Second Institute of Oceanography, Ministry of Natural Resources, Hangzhou, People's Republic of China
[3] Geophysical Fluid Dynamics Laboratory, National Oceanic and Atmospheric Administration, Princeton, NJ 08540, United States of America
[*] Author to whom any correspondence should be addressed.

E-mail: wenxia.zhang@sklec.ecnu.edu.cn

Keywords: coastal hypoxia, climate warming, eutrophication, deoxygenation

Supplementary material for this article is available online

Abstract

The coastal region in east China experiences massive anthropogenic eutrophication, and the bottom water off the Changjiang River Estuary in the East China Sea faces the threat of severe seasonal hypoxia. We find that projected future climate changes will work in parallel with anthropogenic eutrophication to exacerbate current hypoxia and increase shelf vulnerability to bottom hypoxia. We use a coupled physical-biogeochemical regional model to investigate the differences of shelf hydrography and oxygen dynamics between present and future projected states. Model results indicate that the Yellow Sea Cold Water Mass which plays essential roles in nekton migration and shellfish farming practically disappears by the end of the 21st century, and shelf vertical stratification strengthens by an average of 12.7%. Hypoxia off the Changjiang River Estuary is exacerbated with increased (by one month) hypoxia duration, lower dissolved oxygen minima, and significant lateral (202%) and vertical (60%) expansions of hypoxic water. Reduced oxygen solubility, and accelerated oxygen consumption under increased primary production and rising water temperature contribute 42% and 58%, respectively, of bottom dissolved oxygen decrease in the East China Sea. Model results also show increased vertical diffusion of oxygen, despite vertical stratification strengthening, due to increased surface-bottom oxygen concentration gradient associated with increased oxygen release in surface water and exacerbated oxygen consumption in subsurface water.

1. Introduction

Climate warming has caused aquatic dissolved oxygen content to decline due to changes in oxygen solubility, lateral oxygen transport, vertical oxygen exchange, remineralization patterns, and multi-scale nutrient delivery that controls primary production (Justić *et al* 1996, 1997, 2003, Oschlies *et al* 2008, Stramma *et al* 2008, Rabalais *et al* 2010, Schmidtko *et al* 2017). Warming-induced deoxygenation occurs more rapidly in coastal regions than in the open ocean (Chen *et al* 2007, Breitburg *et al* 2018). Declining dissolved oxygen concentrations and the often accompanying acidification can result in habitat displacement within ecosystems and significant changes in marine community niches (Mislan *et al* 2017). Working in parallel with intense anthropogenic activities, warming may worsen coastal ecosystem situations, especially in systems already under the threat of severely seasonal hypoxia (dissolved oxygen, DO < 63 mmol m^{-3}). With the observed enhanced warming effect in recent decades combined with these projected future increases (Bopp *et al* 2013, Kwiatkowski *et al* 2020), evaluation of potential variations at regional to local scales has become increasingly urgent.

The coastal seas in east China consist of the Bohai Sea, Yellow Sea, and East China Sea, each of which have different physical and biogeochemical characteristics that are being affected by warming. The coastal seas in east China have been influenced by severe anthropogenic eutrophication and algal blooms for decades (Li *et al* 2014). Summer bottom dissolved oxygen level shows a rapid decline and approaches hypoxia in recent years in the Bohai Sea (Wei *et al* 2019, Song *et al* 2020), a shallow and semi-closed sea in northeast China. The Yellow Sea, a biologically rich and productive semi-closed marginal sea in east China, is characterized by distinct topography (Fu *et al* 2016). The Yellow Sea Cold Water Mass (YSCWM), located at the central bottom Yellow Sea in summer and characterized by water temperature lower than 12 °C, plays essential roles in nekton migration and shellfish farming (Yin *et al* 2013, Zhao *et al* 2019, Liang *et al* 2020, Zhu *et al* 2020). Long-term deoxygenation has also been observed in the southern Yellow Sea (Wei *et al* 2021). Bottom hypoxia is recurrent in the summer off the Changjiang River Estuary in the East China Sea, one of the well-known hypoxic regions, to form one of the world's largest coastal hypoxia zones (Chen *et al* 2007). The formation and sustainment of seasonal hypoxia off the Changjiang River Estuary is dual-controlled by anthropogenic activities and natural processes (Wang *et al* 2016, Chi *et al* 2017, Zhou *et al* 2017, 2020, Große *et al* 2020).

Climate warming is projected by global climate models to cause severe water temperature increase and deoxygenation in the coastal seas in east China by the end of the 21st century (Bopp *et al* 2013, Kwiatkowski *et al* 2020). Thus, climate warming would exacerbate the shelf hypoxia condition and shrink the habitat of cold-water species (Liang *et al* 2018). Climate warming influences dissolved oxygen concentration through multiple factors. Rising water temperature reduces oxygen solubility, enhances water column stratification, and causes changes in local oxygen production/consumption rates. Changes in river discharge and anthropogenic nutrient loads/concentrations entering the shelf water regulate the strength of vertical stratification and lateral delivery of nutrients to strongly influence the spatiotemporal extent of bottom hypoxia (Zhang *et al* 2021). Precipitation is projected to increase in this region (Li *et al* 2021), which can also strengthen water column vertical stratification. The areal extent of hypoxia in Chinese coastal waters has also been suggested to be sensitive to atmospheric nitrogen deposition based on a global model of coastal oxygen and nutrient dynamics under future projections (Yau *et al* 2020).

Most existing coupled global climate models lack the proper resolution of regional circulation systems critical to regional to local scale mechanisms, making it difficult to quantify variations at regional to local scales (Saba *et al* 2016). Downscaling approaches, the use of high-resolution regional simulations to extrapolate the effects of large-scale climate processes from global scale to regional or local scales, are expected to provide more reliable and robust information at regional to local scales, and have been used to investigate the exacerbated coastal hypoxia in response to climate warming in well-known hypoxic regions like the northern Gulf of Mexico (Lehrter *et al* 2017, Laurent *et al* 2018), the Baltic Sea (Bendtsen and Hansen 2013, Meier *et al* 2017, Saraiva *et al* 2019), and the Chesapeake Bay (Ni *et al* 2019, Tian *et al* 2021). However, high-resolution downscaling projection has not yet been performed for coastal warming and deoxygenation investigations in the coastal seas in east China.

Hence, this study for the first time applies downscaling approach to a coupled physical-biogeochemical regional model. Present day and future projection are performed, the future projection forcing is obtained based on the Geophysical Fluid Dynamics Laboratory (GFDL) climate model CM2.6 high-resolution model (Delworth *et al* 2012). The future-present differences are briefly compared between the high-resolution regional model in this study and the parent global coupled climate model (GFDL-CM2.6) to assess the necessity of downscaling approach for coastal regions with intense anthropogenic activities and complex topography. Then, the present and future projection states of the regional model are compared to investigate the impacts of future condition on shelf properties. The contributions of changes in oxygen solubility, primary production, water column stratification, and oxygen consumption to changes in dissolved oxygen are evaluated. Figure 1 shows a framework of projected physical and biogeochemical changes under climate warming. The purpose of these investigations is to explore the impacts of climate warming on the coastal seas in east China over the 21st century, and provide preliminary base mark for coastal hypoxia management under the background of climate warming.

2. Methodology

2.1. Coupled physical-biogeochemical model

This study used the Regional Ocean Modeling System (ROMS, Shchepetkin and McWilliams 2005) hydrodynamic model and coupled with a biogeochemical model. The hydrodynamic model domain (figure 2(A)) encompasses the entire Bohai Sea, Yellow Sea, East China Sea, part of the Japan Sea and deep region offshore. See text S1 of the supplementary information for brief description of the circulation pattern in the region. The model in this study expanded that of Zhang *et al* (2021) to include 10 rivers along the coast of China (www.mwr.gov.cn/) and 4 rivers along the coast of Korea Peninsula (Kim *et al* 2013). The biogeochemical component is a nitrogen cycle model (Fennel *et al* 2013) expanded to include

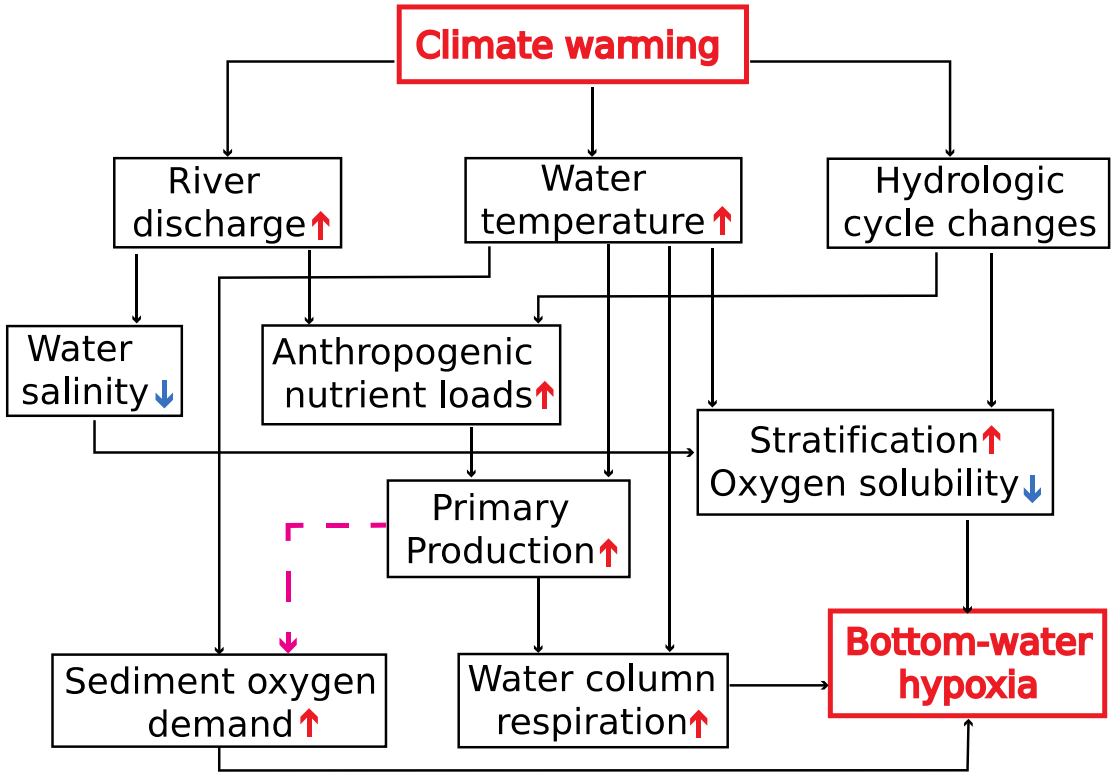

Figure 1. Schematic of the potential physical and biogeochemical changes under climate warming. The dashed arrow indicates the link between primary production and sediment oxygen demand, which actually exists but not accounted for yet in this study.

dynamics of DIP (dissolved inorganic phosphorus) (Laurent *et al* 2017) with a total of 9 variables. See text S2 and table S1 (available online at stacks.iop.org/ERL/17/074006/mmedia) for details of the biogeochemical component.

The initial and open boundary conditions for nutrients were extracted from the climatological monthly World Ocean Atlas 2013 (WOA13, www.nodc.noaa.gov/OC5/woa13/). The Changjiang riverine nutrient concentration was taken from Gao *et al* (2012), the riverine nutrient concentrations for the other nine rivers along the coast of China were taken from the Bulletin of China Marine Environment (http://english.mee.gov.cn), and the riverine nutrient concentrations for the 4 rivers along the coast of Korea Peninsula were taken from Kim *et al* (2013). The East China Sea region is selected as the region shallower than 100 m between 26°N and 33°N (figure 2(B)), because the Changjiang River freshwater discharge and nutrient loads have the most pronounced impacts in this region. Brief description of the model validation is provided in text S3. A full description of the model setup and the validation is provided in Zhang *et al* (2018, 2021, 2022).

2.2. Parent global coupled climate model

The GFDL climate model CM2.6 is a high-resolution global model (Griffies *et al* 2015) that was run with a simple biogeochemical model (Galbraith *et al* 2015, Yamamoto *et al* 2016) in both a preindustrial control scenario keeping CO_2 at preindustrial levels as well as an idealized warming scenario of increased CO_2 at 1% per year to doubling and then continues running for another 10 years. Changes to the coupled atmosphere-ocean-land system include air temperature, precipitation, short-wave radiation, long-wave radiation, and sea level pressure and river discharge (riverine nutrients concentration remains unchanged). Global mean river discharge is projected to increase in the future (Sperna Weiland *et al* 2012). Along the coast in east China, river discharge increases by an average of 18% in the warming scenario. Sea surface temperature over the coastal seas in east China rises by an average of 1.9 °C based on the differences between the warming scenario and the preindustrial control scenario. Note that data of the first 5 years after CO_2 doubled was used to derive the differences between the two scenarios. This temperature rise is consistent with the 2 °C rise of sea surface temperature for the region over the 21st century based on the Earth system models participating in the Coupled Model Intercomparison Project Phase 6 (Kwiatkowski *et al* 2020) and about 1 °C higher than the limit of 2 °C above preindustrial in the Paris Agreement (UNFCCC 2015).

2.3. Model simulations

Two simulations that represent a present condition and a projected future condition are performed. The present simulation is forced by the physical and biogeochemical conditions that are described in

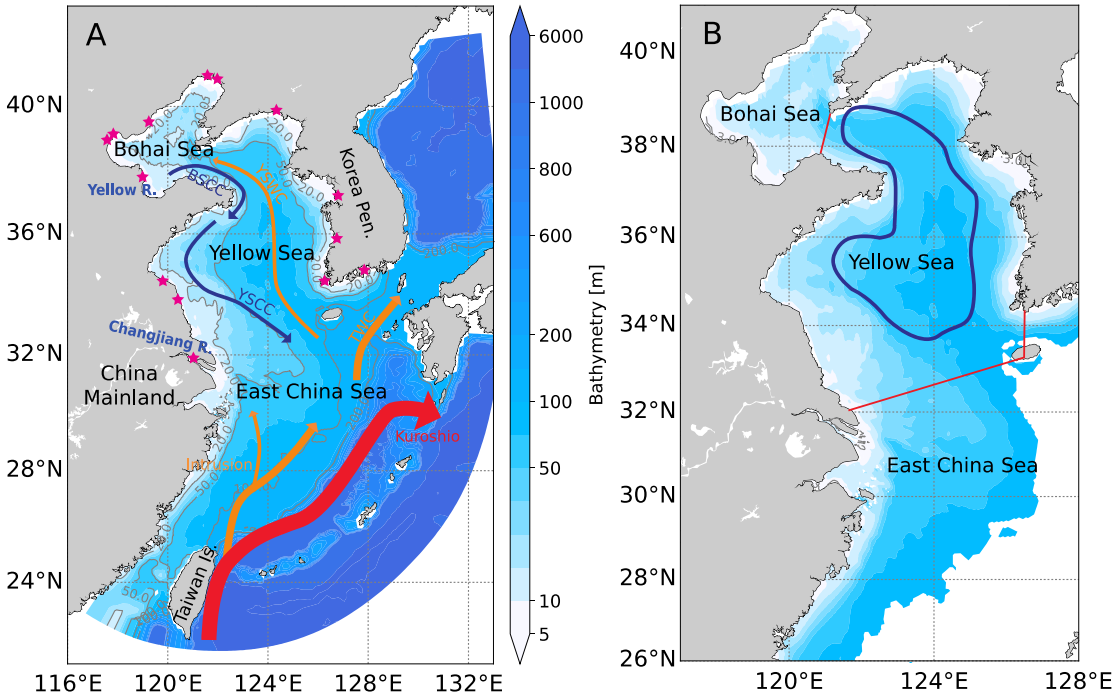

Figure 2. (A) The entire model domain, in which the paths of the Kuroshio current, the Kuroshio subsurface water intrusion are denoted. The red stars denote the locations of multiple rivers that introduce both freshwater and nutrients into the study domain. The Changjiang and Yellow Rivers are labeled. The circulation pattern in the coastal and shelf water is briefly marked. The abbreviations of the currents are for Tsushima Warm Current (TWC), Yellow Sea Coastal Current (YSCC), Yellow Sea Warm Current (YSWC), and Bohai Sea Coastal Current (BSCC). The gray contour lines are 20, 50, 100, and 200 m isobath. (B) The red lines separate the Bohai Sea, the Yellow Sea, and the East China Sea (shallower than 100 m). The thick black isoline denotes the typical location of Yellow Sea Cold Water Mass.

Table 1. Model forcing in the present and future simulations. The dash means no change between present and future simulations. Note that T_w represents water temperature, DO represents Dissolved oxygen concentration, T_a represents air temperature, P represents precipitation, Swrad represents short-wave radiation, Lwrad represents long-wave radiation, Slp represents sea level pressure, and N_c represents Nutrients concentration. WOA13 represents World Ocean Atlas 2013 (WOA13, www.nodc.noaa.gov/OC5/woa13/), while ECMWF represents European Center for Medium-Range Weather Forecasts (ECMWF, www.ecmwf.int/en/forecasts/datasets). Note that 'bias' is the 5 year averaged differences between the two GFDL-CM2.6 scenarios (warming minus preindustrial control).

	Initial/boundary condition								River	
	T_w	Salinity	DO	T_a	P	Swrad	Lwrad	Slp	Discharge	N_c
Present	WOA13	WOA13	WOA13	ECMWF	ECMWF	ECMWF	ECMWF	ECMWF	Observed	Observed
Future	+bias	+bias	+bias	+bias	+bias	+bias	+bias	+bias	+bias	—

the **Model description** subsection. This simulation was initiated in January 2009 and ran for 7 years, and 4-hourly model output since 2011 was analyzed to ensure sufficient spin-up. Model output for 2011–2015 were analyzed and averaged.

The future simulation differs from the present simulation in water temperature, salinity, and dissolved oxygen concentration for initial and boundary conditions, river discharge, and atmospheric forcing including air temperature, precipitation, short-wave radiation, long-wave radiation, and sea level pressure (see table 1 for details). The 5 years-average differences between the two GFDL-CM2.6 scenarios (warming minus preindustrial control) for water temperature (figure S1), salinity (figure S2), and dissolved oxygen concentration (figure S3) are interpolated to the regional model grid. Similarly, the 5 years-average differences between the two scenarios for river discharge and atmospheric forcing are derived. The differences are added to the boundary and initial conditions, river discharge, and atmospheric forcing of the present simulation to force the future projection simulation. Note that riverine nutrients concentration remains unchanged in future projection following GFDL-CM2.6.

3. Results

3.1. General variations under climate warming

Regional model shows a larger magnitude of temperature increase at the surface (+1.6 °C) than the bottom (+1.2 °C) by the end of the 21st century (figures S1(B) and (D)). Temperature increase at the bottom is tightly linked to bathymetry such that larger temperature increases correspond to shallower water depth. Regional model projection indicates that the surface

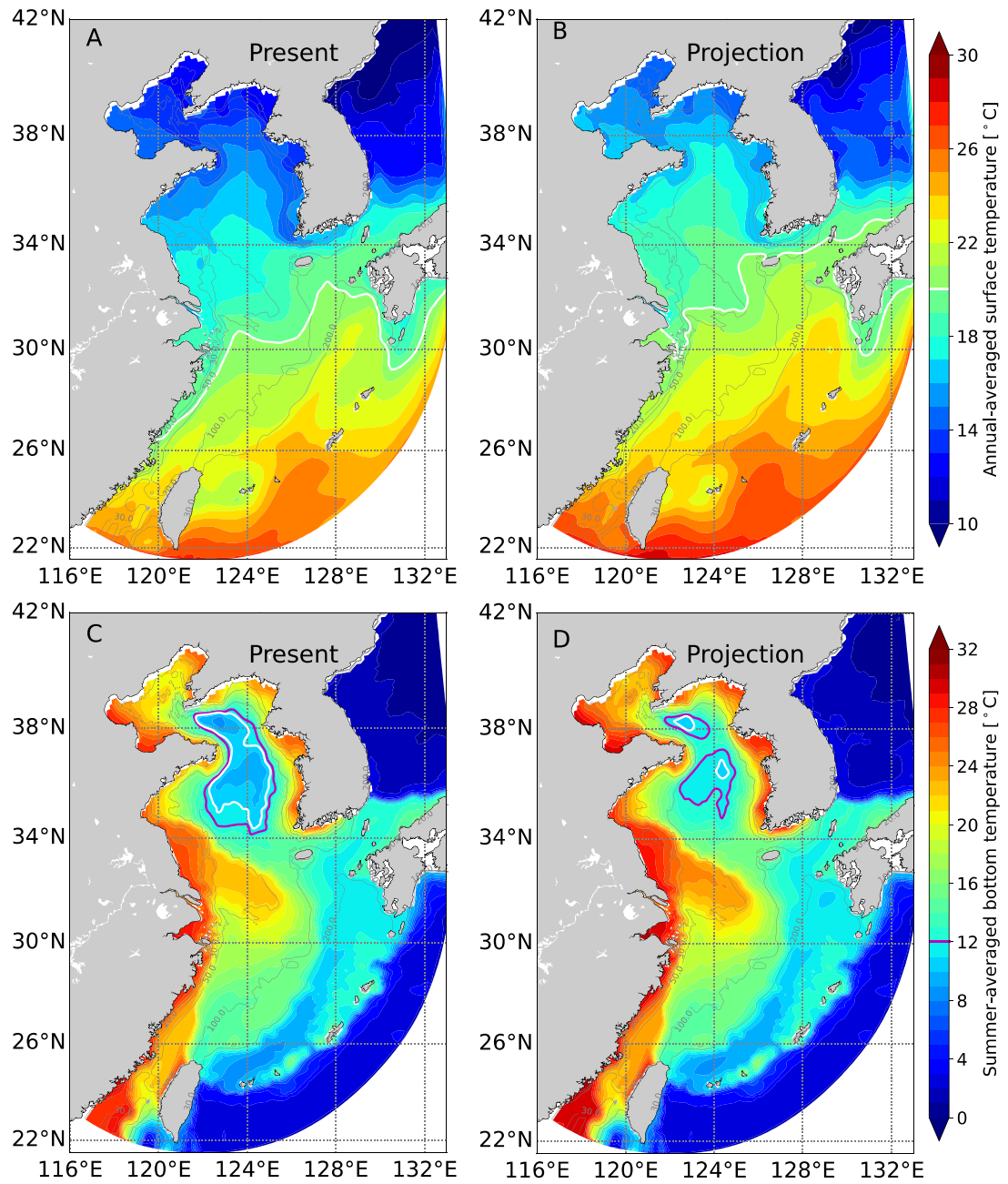

Figure 3. Regional-model-based annual-averaged surface temperature for (A) present, and (B) projection. The white isoline denotes 20 °C isothermal. Regional-model-based summer-averaged bottom temperature for (C) present, and (D) projection. The white and magenta isolines denote 11 °C and 12 °C isothermal, respectively. Note that the 12 °C isothermal line corresponds to the YSCWM. The gray isolines are 20, 30, 50, 100, and 200 m isobath.

20 °C isothermal would migrate northward by over 100 km by the end of the 21st century (figures 3(A) and (B)). The YSCWM at the central bottom Yellow Sea in summer shrinks in the projected future, and water with temperature lower than 11 °C virtually disappears by the end of the 21st century (figures 3(C) and (D)). Freshening (−0.61 psu at the surface and −0.64 psu at the bottom, respectively) associated with riverine input is seen along the coast (figure S2) due to increased river discharge in future projection. Lateral spread of salinity decrease is more significant at the surface than at the bottom (figures S2(B) and (D)). The surface 31 and 32 isohalines would migrate offshore by over 20 km and 40 km, respectively, by the end of the 21st century (not shown).

Bottom water dissolved oxygen shows a larger decrease (−12.4 mmol m^{-3}) than surface water (−7.6 mmol m^{-3}) (figures S3(B) and (D)). The surface dissolved oxygen decrease is tightly linked to topography, such that larger oxygen decrease corresponds to shallower water depth primarily because of a greater increase in temperature (figures S1(B) and S3(B)). Areas under strong influence of riverine input of anthropogenic nutrients experience

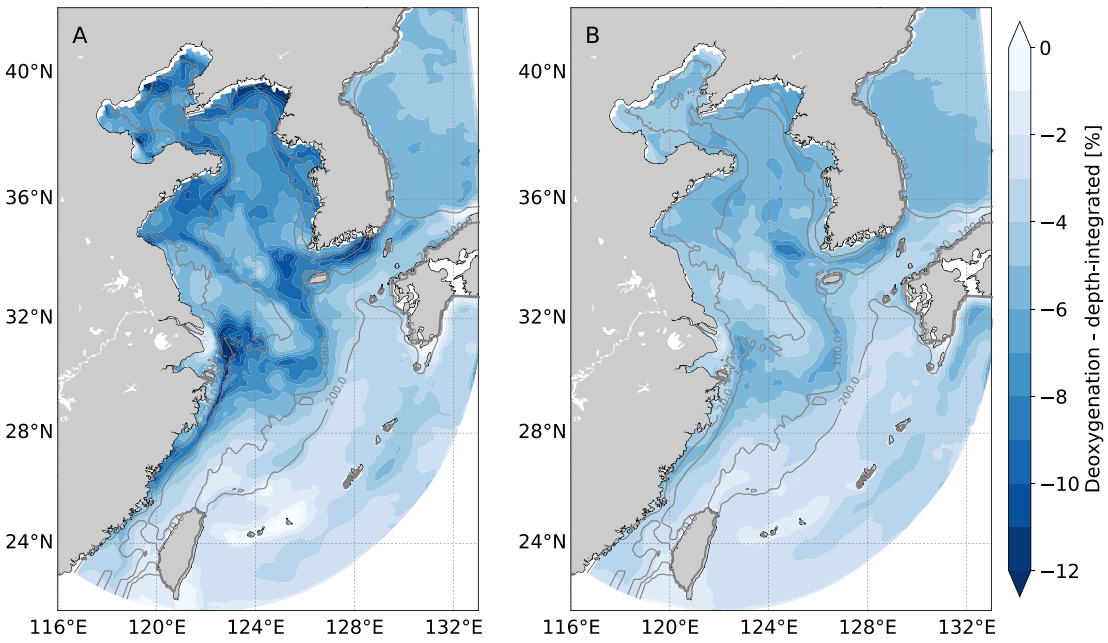

Figure 4. Regional-model-based plan-view of (A) summer-averaged, and (B) annual-averaged future deoxygenation (the decline in depth-integrated oxygen content). The gray isolines are 20, 50, 100, and 200 m isobath.

severe bottom oxygen decrease primarily because of increased primary production and associated organic matter to decompose (figure S3(D)). Severe bottom oxygen decrease is also seen in the central Yellow Sea (figure S3(D)).

Deoxygenation (difference in depth-integral of dissolved oxygen between future projection and present) is seen in the whole domain with a larger magnitude in the coastal region than in the deep, open region (figure 4). The projected future shows that summer-averaged (June–August) dissolved oxygen inventory declines by 6.4% in the shallow region (<200 m) and 3.3% in the deep region, respectively (figure 4(A)). Annual-averaged dissolved oxygen inventory declines by 4.7% in the shallow region and 3.4% in the deep region, respectively (figure 4(B)). Similar to bottom dissolved oxygen decrease as shown in figure S3(D), the areas that are under the influence of riverine input experience severe deoxygenation. Future deoxygenation in the deep region is due to decreased boundary dissolved ocean with warming in the parent model while the relatively more severe deoxygenation in the shallow region is dually controlled by the decreased dissolved oxygen of the boundary condition and the internal model dynamic changes.

3.2. Brief comparisons between the projection of regional model and GFDL CM2.6

The projection-minus-present differences between GFDL and regional model are briefly discussed in text S4. Our regional model results suggest the need for downscaling for robust process level representation of coastal systems. A bottom scheme associated with tidal dissipation is applied to CM2.6, which can influence the surface in shallow regions, especially in regions under intense tidal modulation like the coastal seas in east China. Figures S1 and S2 shows that the coarse bathymetry/vertical representation in CM2.6 leads to a severe underestimate of climate warming induced surface-bottom gradients for temperature and salinity over the continental shelf relative to the regional model. The differences of freshwater spread near the coast between the surface and bottom are not well represented in CM2.6, with the offshore spread of its river plume front being overestimated. In the observed, surface-trapped river plume, freshwater generally spreads offshore at the surface and the offshore-spread of freshwater at the bottom is inhibited by the denser water offshore, and the location of the river plume front are decently captured by the regional model. The resultant differences in temperature, salinity, and biogeochemical components all contribute to the differences in dissolved oxygen decline between CM2.6 and regional model (figure S3).

3.3. Consequences of climate warming

Summer vertical stratification strengthens by 12.7% on average due to the increased water temperature, river discharge, and precipitation in the projected future. The model-based maximum value of vertical density gradient was used to quantitatively represent the strength of bulk stratification. The strengthening magnitude varies from 12% in regions shallower than 75 m to 14% in deeper regions. The future projection

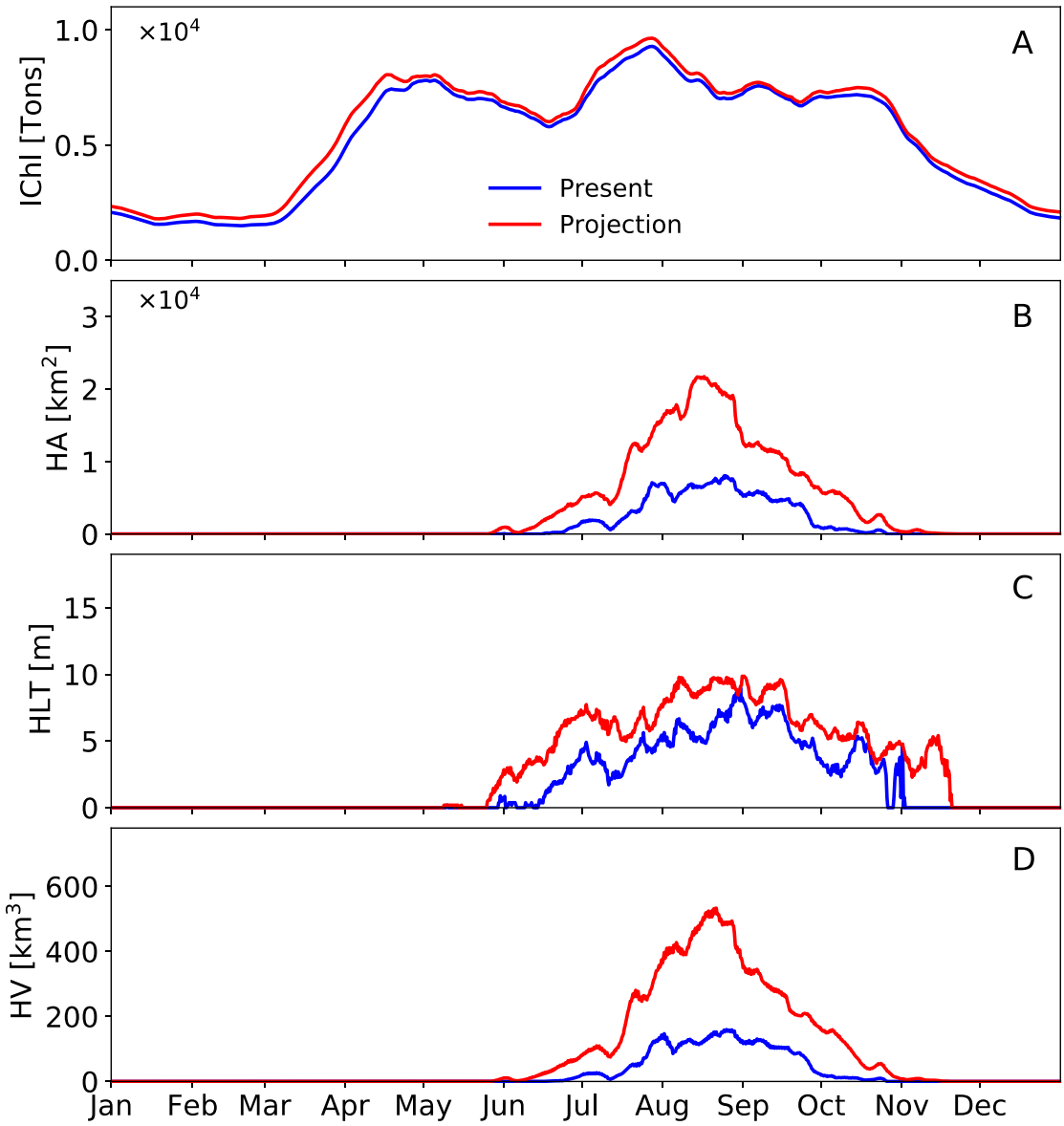

Figure 5. Regional-model-based time series of (A) chlorophyll concentration integral, (B) hypoxic area, (C) hypoxic layer thickness, and (D) hypoxic volume over the region selected in the East China Sea (see figure 2(B)). Note that blue shows present condition, and red shows projection condition.

shows higher local chlorophyll integral (figure 5(A)) as well as spatial expansion of high chlorophyll integral (figures 6(D) and (H)), indicating more oxygen released in the surface water and more oceanic organic matter to consume dissolved oxygen in the subsurface water column. Increased primary production, represented by chlorophyll, in the future projection (figures 5 and 6) is due to the increased nutrient loads associated with increased river discharge and the increased phytoplankton growth rate associated with rising water temperature. Oxygen solubility declines in the projected future. The declined oxygen solubility contributes 74% of bottom oxygen decrease in the deep, open region (>200 m) and 49% of bottom oxygen decrease in the coastal region. Note that the calculation of this contribution was done following Laurent *et al* (2018). The declined oxygen solubility in the future only contributes an average of 42% of bottom oxygen decrease in this region. This indicates that exacerbated biological consumption is a major contributor for bottom oxygen depletion in East China Sea in future projection.

Oxygen budget terms in equation (1) of the supplementary information are quantified for the near-bottom layer (the lower 30% of the water column) in the coastal seas in east China (figure 2(B)). Note that all the terms are normalized by the area of the corresponding subregion. Near-bottom water experiences exacerbated water column respiration and sediment oxygen demand in the projected future (table S2). Sediment oxygen demand accounts for temperature effect but not the change in organic matter deposition (equation (12) of the supplementary information) while water column respiration accounts for

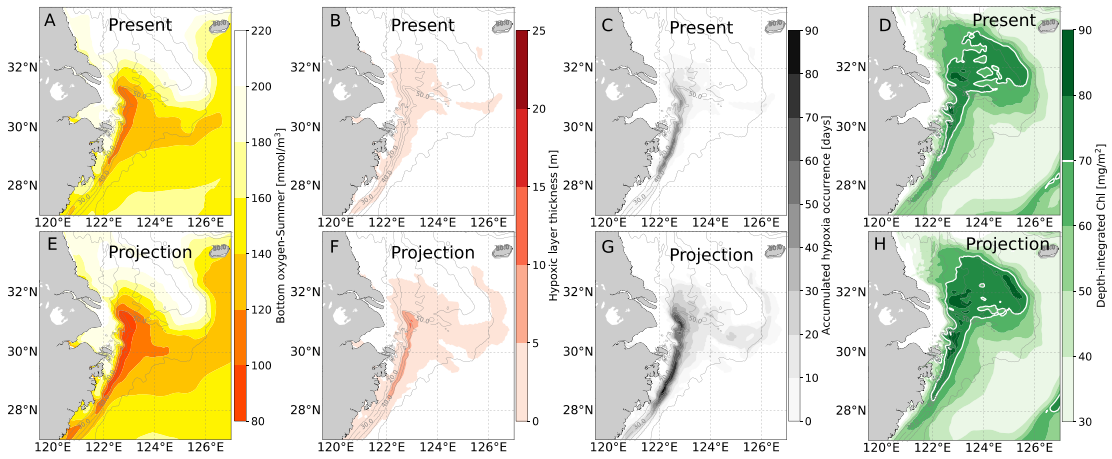

Figure 6. Regional-model-based summer-averaged (A) bottom oxygen concentration, (B) hypoxic layer thickness, (C) accumulated hypoxia occurrence, and (D) depth integrated chlorophyll over the East China Sea for the present condition. The panels (E)–(H) show the identical information for the projection condition. The white isoline in panels (D) and (H) denotes 70 mg m^{-2}. The gray isolines are the 20, 30, 40, 50, and 75 m isobath.

the temperature impact indirectly through the temperature impact on phytoplankton growth and thus organic matter production (equation (3) of the supplementary information). Future water column respiration exacerbates due to increased primary production and organic matter while future sediment oxygen demand exacerbated due to rising water temperature. The strengthening in vertical stratification in the coastal seas in east China is expected to cause a weakening in vertical diffusion induced dissolved oxygen exchange, an important oxygen source for near-bottom water. However, vertical diffusion of dissolved oxygen increases by over 11% in the projected future (table S2). This is because water column respiration and sediment oxygen demand, two leading oxygen sinks, increase by over 10% and 8%, respectively. The exacerbated subsurface oxygen consumption and increased oxygen release in the surface water increase the surface-bottom oxygen concentration gradient, triggering an increased oxygen flux to the near-bottom water.

4. Discussion

The East China Sea is under the pronounced influence of Changjiang River, seasonal oxygen depletion and severe bottom hypoxia occur. Climate warming leads to significant spatiotemporal expansion of seasonal hypoxia off the Changjiang River Estuary in the East China Sea. Bottom hypoxia initiates around half a month earlier and disappears around half a month later in the future projection than those in the present condition (figure 5(B)). Projected future hypoxic area, hypoxic layer thickness, and hypoxic volume increase by an average of 202%, 60%, and 298%, respectively (figure 5). In the future, the East China Sea faces more severely seasonal dissolved oxygen stress with decreased bottom dissolved oxygen minima, expanded hypoxic water distribution, and increased hypoxia sustainment (figure 6). Warming-induced expansions of seasonal hypoxia in this region and those found on the northern Gulf of Mexico show big differences (Lehrter *et al* 2017, Laurent *et al* 2018). The differences could be because of the different dynamics features between the two hypoxic region and different treatments of forcing changes for future simulations.

The exacerbated oxygen consumption and declined oxygen solubility cause the large areal and vertical expansions of hypoxic water in the future projection. Warming-induced oxygen solubility decline contributes 42% of bottom oxygen concentration decrease. Oxygen released via primary production in the lower layer shows small changes (table S2). Changes in horizontal and vertical advections are generally small and cancel each other out (table S2). Water column respiration and sediment oxygen demand are the two major terms that exacerbate oxygen consumption in the future projection, representing nearly 58% of the change in bottom dissolved oxygen concentration in the East China Sea.

Our regional model results suggest that climate warming may have long-term consequences to the coastal ecosystem. The Yellow Sea hosts biologically rich and productive fishing grounds in east China coastal waters, and the YSCWM is of central importance to local fishery (Li *et al* 2006, Fu *et al* 2016, Yang *et al* 2019). The increase of water temperature, the decrease of near-bottom oxygen concentration, and the disappearance of YSCWM may cause changes in fish distribution and migration pattern, and potentially lead to changes in fish species and shrink in fish stocks (Cheung *et al* 2016, Ho *et al* 2020). In comparison with the regional model, GFDL-CM2.6 struggles to represent the vertical temperature gradient and projects higher bottom temperature increase in the

future, especially for the bottom of the Yellow Sea. This indicates that the ability of global model (especially the coarse resolution global models) to estimate the relevant temperature bounds for fish species could be limited at regional to coastal scales. The demersal nekton off the Changjiang River Estuary in the East China Sea has the minimum number of species in summer/early fall (Jiang *et al* 2014), which is highly related to the severe summer hypoxia in this area. The exacerbated condition of bottom hypoxia in the regional future projection would likely degrade biodiversity (Ning *et al* 2011, Chang *et al* 2012).

5. Remaining uncertainties

Extreme events like typhoon/hurricane tend to be more severe in the warming climate with faster wind speed and higher frequency of occurrence (Bhatia *et al* 2018), vertical oxygen exchange can be subsequently strengthened. Multi-scale ocean circulation systems have shifted due to climate warming, and is projected to continue shifting poleward under the warming climate (Grise and Davis 2020). Shifts in ocean circulation can regulate dissolved oxygen concentration by changing lateral oxygen transport and multi-scale nutrient delivery. Besides heat and oxygen fluxes, the variations in Kuroshio subsurface water intrusion would also change the nutrient components over the shelf (Moon *et al* 2021) which subsequently regulate primary production. The variations in shelf wind (strength and direction) and the Kuroshio subsurface water intrusion also play important roles in regulating the spatiotemporal extent of bottom hypoxia off the Changjiang River Estuary (Ni *et al* 2016, Wang *et al* 2017, Zhang *et al* 2021). However, the climate-warming-induced variations in shelf wind speed magnitude and direction, Kuroshio Current itself and the subsequent intrusion into the continental shelf of East China sea are very complex and largely unknown.

One important caveat of the present study is that no variation in shelf wind or Kuroshio subsurface water intrusion is applied to the current version of regional model. The coupled effects of multiple stressors will increase the complexity of mechanism identification. Also, to include variations in shelf wind or Kuroshio subsurface water intrusion without further investigation of these variations would introduce large uncertainties to the current regional model.

More comprehensive investigations downscaling multiple global climate models are needed in the future to project the future state of the shelf and to identify the role of uncertainties. Riverine nutrient concentration could likely change due to variations in anthropogenic activities, introducing further uncertainty. Model parameterization that impacts dissolved oxygen level may also introduce uncertainty to the regional model, for instance, temperature-dependent remineralization rate of organic matter (not considered in this study) or comprehensive parameterization of sediment oxygen demand (simplified in this study). Coastal acidification also occurs concurrently with seasonal bottom hypoxia. Future model development work for the shelf should include carbonate chemistry to investigate shelf water acidification under the pressures of anthropogenic activities and climate change.

6. Conclusions

This study uses a high-resolution coupled physical-biogeochemical model to investigate the impacts of climate warming on the coastal seas in east China. Our model results indicate that global warming will significantly change the shelf hydrographical condition, and the YSCWM would disappear by the end of the 21st century. In the future projection, deoxygenation occurs over the shelf, biogeochemical oxygen consumption exacerbates due to increased primary production and accelerated biogeochemical rates. The declined oxygen solubility and increased biogeochemical oxygen consumption combine to cause increased hypoxia sustainment with lower dissolved oxygen minima, much larger lateral (area) and vertical (thickness) expansions of hypoxic water. Meeting the 2 °C of the Paris Agreement would be expected to reduce the changes between two GFDL scenarios by about half. Our model results suggest the necessity of more comprehensive strategies that take into account not only eutrophication but also climate warming to mitigate coastal hypoxia.

Data availability statement

The data that support the findings of this study are available upon reasonable request from the authors.

Acknowledgments

This work was funded by the Science and Technology Committee of Shanghai Municipal (No. 21ZR1421400), the National Science Foundation of China (No. 41706015), the open fund of State Key Laboratory of Satellite Ocean Environment Dynamics, Second Institute of Oceanography, MNR (No. QNHX2234), and the Innovation Program of Shanghai Municipal Education Commission (Grant No. 2021-01-07-00-08-E00102). Thank Andrew Ross and Elizabeth Drenkard for improving this work.

Conflict of interest

The authors declare no conflicts of interest.

Ethics statement

The authors declare no studies involving human or animal participants.

ORCID iD

Wenxia Zhang https://orcid.org/0000-0002-3757-4089

References

Bendtsen J and Hansen J L 2013 Effects of global warming on hypoxia in the Baltic Sea–North Sea transition zone *Ecol. Modelling* **264** 17–26

Bhatia K, Vecchi G, Murakami H, Underwood S and Kossin J 2018 Projected response of tropical cyclone intensity and intensification in a global climate model *J. Clim.* **31** 8281–303

Bopp L *et al* 2013 Multiple stressors of ocean ecosystems in the 21st century: projections with CMIP5 models *Biogeosciences* **10** 6225–45

Breitburg D *et al* 2018 Declining oxygen in the global ocean and coastal waters *Science* **359** eaam7240

Chang N-N, Shiao J-C and Gong G-C 2012 Diversity of demersal fish in the East China Sea: implication of eutrophication and fishery *Cont. Shelf Res.* **47** 42–54

Chen C-C, Gong G-C and Shiah F-K 2007 Hypoxia in the East China Sea: one of the largest coastal low-oxygen areas in the world *Mar. Environ. Res.* **64** 399–408

Cheung W W, Reygondeau G and Frölicher T L 2016 Large benefits to marine fisheries of meeting the 1.5 °C global warming target *Science* **354** 1591–4

Chi L, Song X, Yuan Y, Wang W, Zhou P, Fan X, Cao X and Yu Z 2017 Distribution and key influential factors of dissolved oxygen off the Changjiang River Estuary (CRE) and its adjacent waters in China *Mar. Pollut. Bull.* **125** 440–50

Delworth T L *et al* 2012 Simulated climate and climate change in the GFDL CM2. 5 high-resolution coupled climate model *J. Clim.* **25** 2755–81

Fennel K, Hu J, Laurent A, Marta-Almeida M and Hetland R 2013 Sensitivity of hypoxia predictions for the northern Gulf of Mexico to sediment oxygen consumption and model nesting *J. Geophys. Res.* **118** 990–1002

Fu M, Wang Z, Pu X, Qu P, Li Y, Wei Q and Jiang M 2016 Response of phytoplankton community to nutrient enrichment in the subsurface chlorophyll maximum in Yellow Sea Cold Water Mass *Acta Ecol. Sin.* **36** 39–44

Galbraith E D *et al* 2015 Complex functionality with minimal computation: promise and pitfalls of reduced-tracer ocean biogeochemistry models *J. Adv. Model. Earth Syst.* **7** 2012–28

Gao L, Li D and Zhang Y 2012 Nutrients and particulate organic matter discharged by the Changjiang (Yangtze River): seasonal variations and temporal trends *J. Geophys. Res.* **117** G4

Griffies S M *et al* 2015 Impacts on ocean heat from transient mesoscale eddies in a hierarchy of climate models *J. Clim.* **28** 952–77

Grise K M and Davis S M 2020 Hadley cell expansion in CMIP6 models *Atmos. Chem. Phys.* **20** 5249–68

Große F, Fennel K, Zhang H and Laurent A 2020 Quantifying the contributions of riverine vs. oceanic nitrogen to hypoxia in the East China Sea *Biogeosciences* **17** 2701–14

Ho C-H, Yagi N and Tian Y 2020 An impact and adaptation assessment of changing coastal fishing grounds and fishery industry under global change *Mitig. Adapt. Strateg. Glob. Change* **25** 1073–102

Jiang Y, Ling J, Li J, Yang L and Li S 2014 Seasonal changes in the demersal nekton community off the Changjiang River estuary *Chin. J. Oceanol. Limnol.* **32** 278–89

Justić D, Rabalais N N and Turner R E 1996 Effects of climate change on hypoxia in coastal waters: a doubled CO_2 scenario for the northern Gulf of Mexico *Limnol. Oceanogr.* **41** 992–1003

Justić D, Rabalais N N and Turner R E 1997 Impacts of climate change on net productivity of coastal waters: implications for carbon budgets and hypoxia *Clim. Res.* **8** 225–37

Justić D, Rabalais N N and Turner R E 2003 Simulated responses of the Gulf of Mexico hypoxia to variations in climate and anthropogenic nutrient loading *J. Mar. Syst.* **42** 115–26

Kim T-W, Lee K, Lee C-K, Jeong H-D, Suh Y-S, Lim W-A, Kim K Y and Jeong H-J 2013 Interannual nutrient dynamics in Korean coastal waters *Harmful Algae* **30** S15–S27

Kwiatkowski L *et al* 2020 Twenty-first century ocean warming, acidification, deoxygenation, and upper-ocean nutrient and primary production decline from CMIP6 model projections *Biogeosciences* **17** 3439–70

Laurent A, Fennel K, Cai W, Huang W, Barbero L and Wanninkhof R 2017 Eutrophication-induced acidification of coastal waters in the northern Gulf of Mexico: insights into origin and processes from a coupled physical-biogeochemical model *Geophys. Res. Lett.* **44** 946–56

Laurent A, Fennel K, Ko D S and Lehrter J 2018 Climate change projected to exacerbate impacts of coastal eutrophication in the northern Gulf of Mexico *J. Geophys. Res.* **123** 3408–26

Lehrter J C, Ko D S, Lowe L L and Penta B 2017 Predicted effects of climate change on northern Gulf of Mexico hypoxia *Modeling Coastal Hypoxia* ed D Justic, K Rose, R Hetland and K Fennel (Cham: Springer) pp 173–214

Li H, Tang H, Shi X, Zhang C and Wang X 2014 Increased nutrient loads from the Changjiang (Yangtz) river have led to increased harmful algal blooms *Harmful Algae* **39** 92–101

Li H, Xiao T, Ding T and Lü R 2006 Effect of the Yellow Sea Cold Water Mass (YSCWM) on distribution of bacterioplankton *Acta Ecol. Sin.* **26** 1012–9

Li Y, Yan D, Peng H and Xiao S 2021 Evaluation of precipitation in CMIP6 over the Yangtze River Basin *Atmos. Res.* **253** 105406

Liang C, Xian W and Pauly D 2018 Impacts of ocean warming on China's fisheries catches: an application of "mean temperature of the catch" concept *Front. Mar. Sci.* **5** 26

Liang Y, Zhao Z, Zhang G, Wang S, Wan A and Liu Q 2020 Distinguishing nutrient-depleting effects of scallop farming from natural variabilities in an offshore sea ranch *Aquaculture* **518** 734844

Meier H E M, Höglund A, Eilola K and Almroth-Rosell E 2017 Impact of accelerated future global mean sea level rise on hypoxia in the Baltic Sea *Clim. Dyn.* **49** 163–72

Mislan K A S, Deutsch C A, Brill R W, Dunne J P and Sarmiento J L 2017 Projections of climate-driven changes in tuna vertical habitat based on species-specific differences in blood oxygen affinity *Glob. Change Biol.* **23** 4019–28

Moon J-Y, Lee K, Lim W-A, Lee E, Dai M, Choi Y-H, Han I-S, Shin K, Kim J-M and Chae J 2021 Anthropogenic nitrogen is changing the East China and yellow seas from being N deficient to being P deficient *Limnol. Oceanogr.* **66** 914–24

Ni W, Li M, Ross A C and Najjar R G 2019 Large projected decline in dissolved oxygen in a eutrophic estuary due to climate change *J. Geophys. Res.* **124** 8271–89

Ni X, Huang D, Zeng D, Zhang T, Li H and Chen J 2016 The impact of wind mixing on the variation of bottom dissolved oxygen off the Changjiang Estuary during summer *J. Mar. Syst.* **154** 122–30

Ning X, Lin C, Su J, Liu C, Hao Q and Le F 2011 Long-term changes of dissolved oxygen, hypoxia, and the responses of the ecosystems in the East China Sea from 1975 to 1995 *J. Oceanogr.* **67** 59–75

Oschlies A, Schulz K G, Riebesell U and Schmittner A 2008 Simulated 21st century's increase in oceanic suboxia by CO2-enhanced biotic carbon export *Glob. Biogeochem. Cycles* **22** GB4008

Rabalais N, Diaz R J, Levin L, Turner R E, Gilbert D and Zhang J 2010 Dynamics and distribution of natural and human-caused hypoxia *Biogeosciences* **7** 585–619

Saba V S *et al* 2016 Enhanced warming of the N orthwest A tlantic O cean under climate change *J. Geophys. Res.* **121** 118–32

Saraiva S, Meier H M, Andersson H, Höglund A, Dieterich C, Gröger M, Hordoir R and Eilola K 2019 Baltic Sea ecosystem response to various nutrient load scenarios in present and future climates *Clim. Dyn.* **52** 3369–87

Schmidtko S, Stramma L and Visbeck M 2017 Decline in global oceanic oxygen content during the past five decades *Nature* **542** 335–9

Shchepetkin A F and McWilliams J C 2005 The regional oceanic modeling system (ROMS): a split-explicit, free-surface, topography-following-coordinate oceanic model *Ocean Modelling* **9** 347–404

Song G, Zhao L, Chai F, Liu F, Li M and Xie H 2020 Summertime oxygen depletion and acidification in Bohai Sea, China *Front. Mar. Sci.* **7** 252

Sperna Weiland F C, Van Beek L P H, Kwadijk J C J and Bierkens M F P 2012 Global patterns of change in discharge regimes for 2100 *Hydrol. Earth Syst. Sci.* **16** 1047–62

Stramma L, Johnson G C, Sprintall J and Mohrholz V 2008 Expanding oxygen-minimum zones in the tropical oceans *Science* **320** 655–8

Tian R, Cerco C F, Bhatt G, Linker L C and Shenk G W 2021 Mechanisms controlling climate warming impact on the occurrence of hypoxia in Chesapeake Bay *J. Am. Water Resour. Assoc.* 1–21

UNFCCC Adoption of the Paris agreement *Report* No. FCCC/CP/2015/L.9/Rev.1 (available at: http://unfccc.int/resource/docs/2015/cop21/eng/l09r01.pdf)

Wang B, Chen J, Jin H, Li H, Huang D and Cai W 2017 Diatom bloom-derived bottom water hypoxia off the Changjiang estuary, with and without typhoon influence *Limnol. Oceanogr.* **62** 1552–69

Wang H, Dai M, Liu J, Kao S-J, Zhang C, Cai W-J, Wang G, Qian W, Zhao M and Sun Z 2016 Eutrophication-driven hypoxia in the East China Sea off the Changjiang Estuary *Environ. Sci. Technol.* **50** 2255–63

Wei Q, Wang B, Yao Q, Xue L, Sun J, Xin M and Yu Z 2019 Spatiotemporal variations in the summer hypoxia in the Bohai Sea (China) and controlling mechanisms *Mar. Pollut. Bull.* **138** 125–34

Wei Q, Xue L, Yao Q, Wang B and Yu Z 2021 Oxygen decline in a temperate marginal sea: contribution of warming and eutrophication *Sci. Total Environ.* **757** 143227

Yamamoto A *et al* 2016 Cross-frontal processes and the transport of physical and biogeochemical tracers into the North Pacific and North Atlantic subtropical gyres *Am. Geophys. Union* **2016** B44B–0384

Yang Y, Li K, Du J, Liu Y, Liu L, Wang H and Yu W 2019 Revealing the subsurface Yellow Sea cold water mass from satellite data associated with typhoon Muifa *J. Geophys. Res.* **124** 7135–52

Yau Y Y, Baker D M and Thibodeau B 2020 Quantifying the impact of anthropogenic atmospheric nitrogen deposition on the generation of hypoxia under future emission scenarios in Chinese coastal waters *Environ. Sci. Technol.* **54** 3920–8

Yin J, Zhao Z, Zhang G, Wang S and Wan A 2013 Tempo-spatial variation of nutrient and chlorophyll-α concentrations from summer to winter in the Zhangzi Island Area (Northern Yellow Sea) *J. Ocean Univ. China* **12** 373–84

Zhang W, Dunne J P, Wu H, Zhou F and Huang D 2022 Using timescales of deficit and residence to evaluate near-bottom dissolved oxygen variation in coastal seas *J. Geophys. Res.* **127** e2021JG006408

Zhang W, Moriarty J M, Wu H and Feng Y 2021 Response of bottom hypoxia off the Changjiang River Estuary to multiple factors: a numerical study *Ocean Modelling* **159** 101751

Zhang W, Wu H and Zhu Z 2018 Transient hypoxia extent off Changjiang River Estuary due to mobile Changjiang River plume *J. Geophys. Res.* **123** 9196–211

Zhao Y, Zhang J, Lin F, Ren J S, Sun K, Liu Y, Wu W and Wang W 2019 An ecosystem model for estimating shellfish production carrying capacity in bottom culture systems *Ecol. Modelling* **393** 1–11

Zhou F *et al* 2017 Investigation of hypoxia off the Changjiang Estuary using a coupled model of ROMS-CoSiNE *Prog. Oceanogr.* **159** 237–54

Zhou F *et al* 2020 Coupling and decoupling of high biomass phytoplankton production and hypoxia in a highly dynamic coastal system: the Changjiang (Yangtze River) Estuary *Front. Mar. Sci.* **7** 259

Zhu Y, Zhang Z, Reygondeau G, Chu J, Hong X, Wang Y and Cheung W W 2020 Projecting changes in the distribution and maximum catch potential of warm water fishes under climate change scenarios in the Yellow Sea *Divers. Distrib.* **26** 806–17